Experimental and numerical study on the thermal performance of polycarbonate panels

ČEKON, M.; ŠIKULA, O.

Journal of Building Engineering
Volume 32, November 2020, 101715, Pages 1-14

ISSN: 2352-7102

DOI: https://doi.org/10.1016/j.jobe.2020.101715

Accepted manuscript

HIGHLIGHTS:

- The thermal performance of polycarbonates is obtained experimentally and numerically
- A detailed characterization of the equivalent thermal conductivity is provided
- Equivalent thermal conductivity is not significantly affected by the inclination angle
- Numerical 3D CFD models are developed to quantify the heat transfer characteristics
- Low-e application in PC reduces the equivalent thermal conductivity from 24% to 43%

Experimental and numerical study on the thermal performance of polycarbonate panels

ABSTRACT:

Polycarbonate panels are a specific type of transparent insulation material that can be usefully integrated in building envelope structures. As the applications for such systems are increasing, it was necessary to analyze in detail data for materials which are already available to improve their thermal performance. In this paper the experimental campaign was based on the detailed characterization of the equivalent thermal conductivity parameters of several representative polycarbonate panels. The dependence of the equivalent thermal conductivity on the temperature and different angles of inclination are analyzed. Increasing the angle of the investigated polycarbonate panels changed the thermal conductivity parameters to a very minor degree. On the other hand, the effect of temperature on the thermal properties is proved to be significant and the conversion temperature coefficient is provided in this regard. The computational fluid dynamics (CFD) numerical analysis is employed to validate three-dimensional CFD models and simulate the thermal performance of low-e panels for it to theoretically improve their overall thermal parameters. When applying low-e functionality, depending on the type of polycarbonate panel, the equivalent thermal conductivity was found to range from 0.03750 W/(m·K) to 0.04172 W/(m·K), representing a reduction ranging from 43% to 24%.

Keywords: Transparent insulation material; Polycarbonate panels, Low emissivity; Model validation; Computational fluid dynamics; Radiation heat transfer

1 INTRODUCTION

The reduction of building energy consumption is one of the key issues that need to be solved by the contemporary construction industry. One of the way is the improvement of the thermal performance of building envelope. There are various promising ways of improving the thermal performance of building materials and systems by enhancing their thermal insulation parameters. Thus, the development and evaluation of different technical solutions and the integration of innovative solutions in building envelopes are continually relevant research challenges [1][2]. In this relation, the improved thermal insulation achieved by integrating transparent insulation materials (TIMs) into building envelopes can ultimately affect the overall energy efficiency of buildings [3]. A TIM combines two functionalities in one material. Basically, it can reduce heat loss by providing a certain level of thermal resistance while effectively transmitting solar energy and influencing other aspects of the building environment. This characteristic can reduce heat losses and efficiently transfer solar heat energy. As a result, continuous efforts are being made in the field of TIM development [4], which demonstrates that transparent insulation systems are promising technologies for insulation and the utilization of passive solar energy strategies, or even daylighting [5]. At this stage, research and development concerning improvements to both new and existing materials for building integration can be fostered through the use of numerical simulation tools, though these need to be properly verified at the initial stage.

The usefulness of TIMs has been widely studied and developed worldwide over the past few decades [6] predominantly with regard to their application in the case of solar thermal collectors [7][8]. However, their integration in building envelopes has also seen some attention [9][10]. Furthermore, there also have been several studies focused on solar walls where TIMs have replaced the original glazing elements [11]. Their integration in building facades is still under development, even though commercial products already exist [4]. A wide range of types of TIM have already been introduced and characterised in terms of both thermal and optical behaviour, with research being done into the benefits that may be obtained through their application to buildings [12][13]. They are typically employed in glazing systems, especially those that are aerogel-filled or utilize a specific capillary system.

Most manufacturers use polycarbonate and silica aerogels to produce TIMs, though other materials and solutions are also possible. Polycarbonate systems have improved thermal performance because of multiwall polycarbonate panels with an air space in between. These multiwall polycarbonate systems can be further enhanced by filling them with capillary structure in order to obtain a transparent insulation system with lower equivalent thermal conductivity values [4]. Several multiwall panels made from co-extruded polycarbonate and intended for use in buildings have already been investigated in order to study the thermal, optical and solar properties of polycarbonate panels with a cellular structure and its different cell geometric characteristics [14][15]. The presence of air cavities within the polycarbonate panel assures good thermal insulation, though the air cavities can be filled by, e.g. granular silica aerogel to further improve the thermal performance [16][17]. In this case, the thermal transmittance can be reduced by about 45% to 70% when compared to empty polycarbonate panels. According to the existing research, it is evident that incorporating aerogels in glazing at the structural level provides better thermal insulation [18][19]. Aerogel is considered one of the most promising materials for insulation given its very low thermal conductivity [20][21]. Another perspective research approach can be deemed suitable for building application in combination with Phase Change Materials, where latent thermal energy storage effect is employed [22][23]. Back in the improved thermal parameters of polycarbonate development, further progress which was recently investigated involved the application of a transparent insulating medium containing gas bubbles with the aim of affecting both radiation heat transfer and thermal conduction. Detailed theoretical models have been developed [24] to analyse the most effective thermal conductivity parameters. Further innovations can be based on the effect of coupled radiation - natural convection heat transfer to improve overall thermal parameters. In this relation, one potential solution that could theoretically improve the thermal performance of polycarbonate panels whilst maintaining their solar transmittance is to enhance a TIM by adding a low-e material to the inside surface of cavities of the whole panel system. This research area is important as the conditions experienced by a building element that incorporates conventional heat transfer are significantly different to those that are based on radiative heat applications. Experimental results have demonstrated that with this technology an improvement in envelope performance is achievable [25]. In particular, a reduction of ~18% in equivalent conductivity was measured in hollow bricks [26]. This method of applying a low-e coating could become a simple and currently available way to improve the thermal performance of hollow bricks [27][28]. Hollow bricks with vertically oriented cavities are widely used in the present-day building industry in order to reduce heat transfer through walls [29].

In real-world applications, the integration of a more complex structure within the air cavity of building materials can have a significant effect on free convection and the long-wave radiation heat transfer. These aspects need to be considered in order to accurately predict thermal performance. The effect of natural convection on the heat transfer in the air cavity systems depends essentially on the angle of inclination from the direction of gravitational acceleration. However, most material parameters are typically determined in the sample´s horizontal position which is perpendicular to the gravitational acceleration. In this relation, the equivalent thermal conductivity of hollow building components in the vertical direction (parallel to the gravitational acceleration) is of high importance in the case of specific two-dimensional or three-dimensional thermal bridges, where a considerable vertical heat flow may additionally appear [30]. This is significantly dependent on other specific aspects such as overall material size, boundary conditions, the final placement of the material within the building envelope, etc. It also specifically corresponds to the fact that when components cannot be treated as homogeneous (such as when the structure is made of different materials or when the heat transfer is two- or three-dimensional), different approaches are needed to accurately evaluate their thermal resistance: numerical evaluations can be useful, but they need to be integrated via experimental validations [16]. Many experimental and numerical studies have emphasized the effect of surface radiation on natural convection in cavities. However, most of them focus on fundamental scales of heat transfer [31]. Overall, the surface radiation from the cavity walls at different emissivities affects the overall heat transfer and flow behavior in the cavity. The radiative interaction between the walls of the cavity and its effects on natural convection heat transfer for different tilt angles are of great importance in the design of some specific systems [32]. Differences in cavity orientation play a decisive role with regard to flow and heat transfer [33].

For many building applications of thermal engineering field, a complex heat transfer mechanism in closed air cavity systems can be effectively identified based on its equivalent thermal conductivity parameters. This can be usefully applied when coupled transient radiation - natural convection heat transfer across polycarbonate panels is considered. In this paper the experimental campaign was focused on obtaining data in the laboratory using experimental measurements and based on the detailed characterization of the equivalent thermal conductivity parameters of existing polycarbonate multiwall system. This research study will present a detailed experimental analysis of the thermal performance of several representative polycarbonate panels under various steady-state conditions specifically analysed at various angles of inclination. The experimental results will be analysed in order to identify the dependence of equivalent thermal conductivity on the temperature and angle of inclination. In addition, the effect of the orientation of air cavities both in vertical and horizontal arrangements will be analyzed. When such cavities are installed in a structure, they are most typically arranged in a vertical orientation. However, so far attention has not been paid to applications where cavities are arranged in the horizontal orientation. This variant also needs to be examined with regard to the possibility of using polycarbonate panels in solar wall concepts [10] where the horizontally oriented arrangement can significantly contribute to the selective function of their solar transmittance [15].

2 METHODOLOGICAL APPROACH, MATERIALS AND METHODS

The key aim of this study is to investigate the thermal properties of polycarbonate panels, which are primarily based on a multi-layered structure with a focus on different geometries and to provide numerically their thermal optimization based on low-e effect. The experimental results will be used for the validation of the results which were obtained computationally. In this case, the simulation results will provide data about the basic models for the reliable prediction of the thermal performance of the newly introduced PC panels with low-e. These were used to investigate equivalent thermal conductivity across the whole extent of the model, involving emissivity changes, variations in angles of inclination and environmental conditions (varying temperature gradients).

The main structure of this study lies in:

- the analysis of the thermal performance of existing multiwall PC panels,
- the use of the CFD approach to validate results obtained computationally,
- the theoretical improvement of the thermal performance applying of low-e material.

The methodology relies on:

i. The detailed characterization of equivalent thermal conductivity: guarded hot plate and heat flow measurement tests were conducted,
ii. Thermal performance modelling using a validated CFD simulation model based on experimental measurements.
iii. Thermal optimization of PC panels with low-e effect applied to their internal walls.

The samples for laboratory analysis were prepared directly from existing PC systems: two multiwall systems with different internal structures were tested via the heat flow meter (HFM) method, and another two panels via the guarded hot plate (GHP) method. The PC samples were prepared with particular dimensions specifically needed for the heat flow measurements, which means that both 600 mm x 600 mm (HFM) and 300 mm x 300 mm (GHP) samples were tested. Table 1 shows the measured samples and provides a typical description. The main difference between them lies in their overall thickness and the structure of their internal division. Practically all of the panels consist basically of rectangular cells, though these are of different sizes, while two of the panels also have several cells which are divided diagonally. PC10 is the simplest type. It consists of two walls and an internal structure which is formed from rectangular cells with the dimensions 9.9 x 10.1 mm. PC20 consists of seven walls forming a basic cell with the dimensions 16.15 x 3.45 mm, which is repeated six times in total. PC25 has two consecutive cells of 9.95 x 12.45 mm which are also divided diagonally, and the average width of the air layer is 6.225 mm. PC32 is the most comprehensive system, as it is a combination of all previous types. The narrowest rectangular geometry with the dimensions 19.95 x 4.45 is used from the outside sides, and subsequently a cell divided diagonally with a width of 8.5 mm is used. In the centre a rectangular cell with a width of 6 mm is used again. The average width of this system is 4.56 mm.

Table 1: Polycarbonate panels.

Sample	Type	Thickness [mm]	Weight [kg.m^{-2}]	Declared U value [34] [W.m^{-2} K^{-1}]	Decl. equivalent thermal conductivity [34][W.m^{-1} K^{-1}]
PC10	Clear 2walls	10.3	1.7	3.0 (*0.165**)	0.06242
PC20	Clear 7walls	20.7	3.0	1.6 (*0.457**)	0.04529
PC25	Clear 3walls /diagonals	25.1	3.4	1.6 (*0.457**)	0.05493
PC32	Clear 6walls combined	32.1	3.6	1.3 (*0.601**)	0.05408

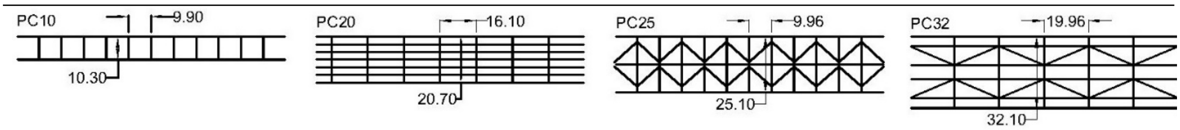

3 EXPERIMENTAL MEASUREMENTS

As the characterization of the thermal insulation properties of construction materials represents a fundamental step in building insulation assessment [30], one of the key assumptions for an experimental approach is based on appropriately quantifying the angular thermal property of the analyzed materials. This is particularly important when air cavities are predominantly employed in the material structure so as an effect on free convection and the long-wave radiation heat transfer may play a decisive role.

Thermal properties were measured using two methods (Table 2) according to EN 12667 [33] with the use of TLP 300-DTX-1P and FOX 630 Rotational devices. The first instrument employs the GHP method, measures thermal resistance and calculates equivalent thermal conductivity in accordance with the ISO 8302 standard [36]. The measuring inaccuracy is ±3% while reproducibility is given at the level of ±1%. The second device, which is based on HFM method stated in ISO 8301 [37], was primarily used to investigate the dependence of thermal conductivity on the tilt angle of the sample and cavity orientation. The absolute thermal conductivity accuracy is ±1% while reproducibility is given at the level of ±0.5%. Since most material parameters are usually determined from samples which are in the horizontal position, when air cavities are integrated in the material the effect of increasing the material's tilt may make a significant contribution to the total heat transfer via the inner structure of such an element. The aim is to measure the sample as if it were realistically placed in the structure of a building (horizontally e.g. in the flat roof, vertically in the wall and at a certain angle as for the pitched roof). This can particularly affect a convective heat transfer. The FOX 630 measuring device thus enables the measurement of heat flow for different sample tilt angles and so the identification of the influence of combined heat transfer through various polycarbonate structures. For the purposes of these measurements various temperature gradients were tested at three mean temperatures in three testing positions (0°, 45° and 90°) for both horizontal (H) and vertical (V) air cavity orientations (Fig. 1). Fig. 1 presents both the cavity orientation (H and V) of each tested sample and angle of inclination (0°, 45°and 90°).

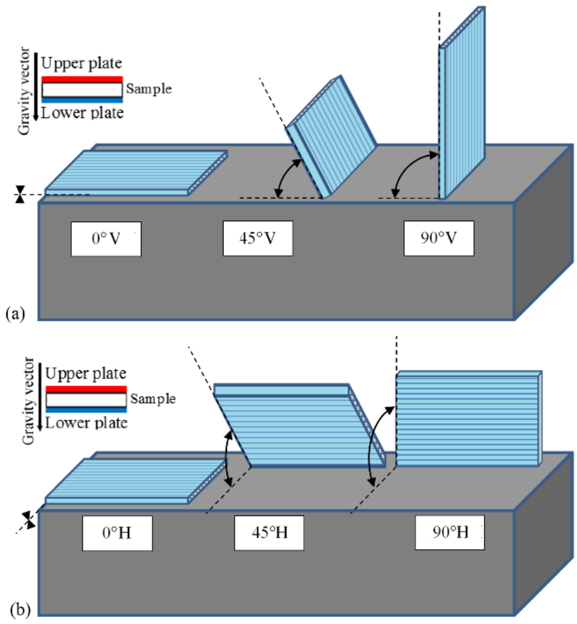

Fig. 1. Tested angles of inclination and cavity orientation of PC samples via HFM tests; (a) vertical V and (b) horizontal H cavity orientation

Table 2: Provided equivalent thermal conductivity measurements and boundary conditions.

Test	GHP	HFM
Mean temperature	10°C, 20°C, 30°C	10°C, 20°C, 30°C
Temperature gradient	10K	10K, 20K, 30K
Angle of inclination	0°	0°, 45°, 90°
Cavity orientation	n/a	H and V
PC samples	PC10, PC20, PC25, PC32	PC25, PC32
Test apparatus	Taurus TLP 300 DTX-1	FOX 630 Rotational

3.1 *Guarded hot plate tests*

The equivalent thermal conductivity of the tested panels was first measured using the guarded hot plate (GHP) test in accordance with the ISO 8302 standard [36]. The thermal resistance of the test sample (1) was calculated from the heating power *q* through the measured surface *A* for the temperature difference between the surfaces of the sample *ΔT*. Finally, the equivalent thermal conductivity coefficient λ_{ekv} was calculated based on the thickness of the material (2).

$$R = \frac{\Delta T \times A}{q} \qquad [(m^2 \cdot K)/W] \qquad (1)$$

$$\lambda_{ekv} = \frac{d}{R} \qquad [W/(m \cdot K)] \qquad (2)$$

According to ISO 10456 [41], the temperature conversion factor of two test conditions can be carried out in terms of the relation (3) and the conversion coefficient for temperature (4) can be derived from the measurement results.

$$\lambda_2 = \lambda_1 \, . \, F_T \qquad (3)$$

$$F_T = \mathrm{e}^{f_T \, . \, (T_2 - T_1)} \qquad (4)$$

The testing of each sample included repeated measurements at three different mean temperatures of 10, 20 and 30° C and temperature gradient of 10 K. The equivalent thermal conductivity of the four tested materials at these three measurement points and conversion of thermal values between them according to [41] is shown in Table 3. The measured thermal conductivity first depends on the structure and arrangement of the inner walls of each system. In general, it is true that panels divided by other internal walls attain lower thermal conductivity values. This finding confirms the initial assumptions. In all cases, the thermal performance decreases at higher mean temperatures. In other words, a higher sample temperature means the material exhibits increased thermal conductivity corresponding to the radiation heat exchange in cavities that is ruled by the third power of the cavity temperature. The last column of Table 3 shows a comparison of the results with the declared value. The comparison of results from various registered laboratories is defined by the European group Keymark [38] in order to ensure consistency between them. A mean temperature of 10 °C ± 1.5% is used with regard to the reference material. Based on the Keymark rules, a mean temperature of 10° C was used for the comparison with the declared value; the last column shows the relative difference between both values. The lowest difference of 6.6% is for the simplest double-walled system PC10, while the greatest, 17.4%, is for the PC25 panel. In connection with the effect of different temperatures on the thermal conductivity, Berardi and Naldi [39] carried out, for example, a revealing experimental study focused on the influence of thermal conductivity on the temperature function which mainly occurs in real situations and applications within a building envelope. Special attention was paid to highly effective polyisocyanurate foam (PIR) -based thermal insulation for which this material exhibits a strongly non-linear dependence between conductivity and temperature conditions. Surprisingly, the values obtained at an average temperature of - 20 °C correspond to a conductivity of up to around 0.04 W / (m·K). Another very similar and even more significant study is the temperature dependency effect of the thermal conductivity that was found for Vacuum Insulation Panels [40]. This indicates that in the context of the rapidly developing research and development that is under way concerning new materials, it is especially necessary to examine them under marginal (particularly temperature) conditions beyond those which are normally tested.

Table 3. Material parameters obtained by the TLP 300-DTX-1P apparatus (GHP)

	Equivalent thermal conductivity at mean temperature [W/(m . K)]					Declared values [W/(m . K)] [34]	
	10 °C (15°C – 5°C)	F_T f_T	20 °C (25°C – 15°C)	F_T f_T	30 °C (35°C – 25°C)	-	%
PC10	0.0668 ± 0.0021	1.0659 0.0064	0.0712 ± 0.0021	1.0716 0.0069	0.0763 ± 0.0023	0.06242	6.56
PC20	0.0527 ± 0.0016	1.0455 0.0045	0.0551 ± 0.0016	1.0563 0.0055	0.0582 ± 0.0017	0.04529	14.06
PC25	0.0665 ± 0.0020	1.0556 0.0054	0.0702 ± 0.0021	1.0712 0.0069	0.0752 ± 0.0022	0.05493	17.40
PC32	0.0601 ± 0.0018	1.0549 0.0053	0.0634 ± 0.0019	1.0789 0.0076	0.0684 ± 0.0020	0.05408	10.02

3.2 *Heat flow meter tests*

The principle behind the measurement is that a constant temperature difference is forced to exist between the upper and lower plates of the test apparatus in order to perform the measurement of heat flow and surface temperatures after the achievement of steady-state conditions. The equivalent thermal conductivity is then calculated using the following equation (5).

$$\lambda_{eq} = \frac{\mathrm{d} \cdot |q|}{\lfloor T_{up} - T_{low} \rfloor} \tag{5}$$

where λ_{eq} is the equivalent thermal conductivity, d is the sample thickness, q is the specific heat flow, and T_{up} and T_{low} are the upper and lower plate temperatures, respectively.

The FOX 630 measurement apparatus consists of a single sample HFM with a guarded ring equipped with two plates containing heat flow meter sensors (with a measurement area of 300 x 300 mm) placed above and below the measured specimen.

The nine test setpoints TS (Table 4) maintained the temperature gradients of 10 K, 20 K and 30 K at three different mean temperatures. This means that three temperature gradients were specifically tested along with three different mean temperature setpoints at the lower and upper plates. Test setpoints TS_5 and TS_6 were measured so that the heat flow corresponded against to the direction of gravity. All the others were measured with heat flow in the direction to gravity. The main objectives of this advanced analysis were:

- To investigate the dependence of the thermal performance of tested components on the angle of inclination,
- To analyse the influence of air cavity orientation on thermal properties,
- To provide a detailed thermal characterization for it to verify the numerical simulations.

Table 4: Test setpoints and boundary conditions.

Test setpoint	TS_1	TS_2	TS_3	TS_4	TS_5	TS_6	TS_7	TS_8	TS_9
Mean temperature [°C]		~ 10			~ 20			~ 30	
Temperature gradient [K]	~ 10	~ 20	~ 30	~ 10	~ 20	~ 30	~ 10	~ 20	~ 30
Upper setpoint [°C]	~ 15	~ 20	~ 25	~ 25	~ 10	~ 5	~ 35	~ 40	~ 45
Lower setpoint [°C]	~ 5	~ 0	~ -5	~ 15	~ 30	~ 35	~ 25	~ 20	~ 15
Measurement arrangement	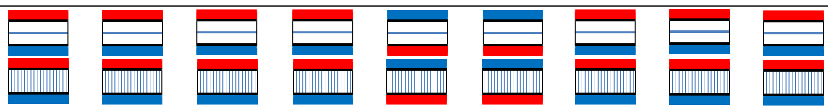								

This leads to the further use of the numerical model to explore the heat transfer characteristics of PC multiwall systems, as well as to the performance of further component optimization studies, e.g. concerning low-e applications.

3.3 *Measurement results*

In this section, the results of measurements performed using the heat flow method are presented for the two coarsest and most complex panels with regard to their internal division (for PC25 and PC32 separately). These were conducted for both the vertical (V) and the horizontal (H) air cavity orientations.

The results presented in Fig. 4 identify the equivalent thermal conductivity values measured for the PC25 panel for all temperature conditions and positions grouped at three setpoints. In general, identical values were recorded for the mean temperature of 10 °C during measurements in the horizontal position and the inclination of the sample caused an increase of 1%. A similar result was also achieved for the mean temperature of 30 °C, but the change in the mean temperature from 10 °C to 30 °C resulted in an increase in the relative value from 0.06457 W / (m·K) to 0.07329 W / (m·K), which represents a difference of approximately 12% in total. If the temperature gradient is raised in the direction opposite to that of gravity, the values are practically identical and the effect of the inclination of the samples does not manifest itself at all. Additionally, the effect of the orientation of air cavities is not demonstrated in any of the tested scenarios. Generally, the lowest equivalent thermal conductivity (0.06457 W / (m·K)) was obtained at a temperature gradient of 10 K (TS_1) when measured in the horizontal position, while the highest (0.07356 W / (m·K)) was gained at the highest temperature gradient of 30 K and a sample inclination of 45° (TS_9); the difference in the relative value was about 12 %. Fig. 5 presents the equivalent thermal conductivity results for the PC32 panel for all setpoints separately. Just as in the case of sample PC25, the values measured in the horizontal position and at a mean temperature of 10 °C are generally identical, and the inclination of the specimen also causes a maximum increase of 1%. This is a negligible value. Similar results are also achieved for the mean temperatures of 30 °C and 20 °C for TS_4, though the change in the mean temperature from 10 °C to 30 °C results in the growth of the relative value from 0.05797 W / (m·K) to 0.06605 W / (m·K), which is a 12% difference. In all of the tested scenarios, the orientation of air cavities with regard to their geometry, structure and particularly size was not recorded as having an effect. Generally, the lowest equivalent thermal conductivity (0.05797 W / (m·K)) was achieved for the temperature gradient 10 K (TS_3) measured in the horizontal position, while the highest (0.06620 W / (mK)) was obtained for the highest temperature gradient of 30K and a sample inclination of 45° (TS_9); the difference in the relative value was around 12%.

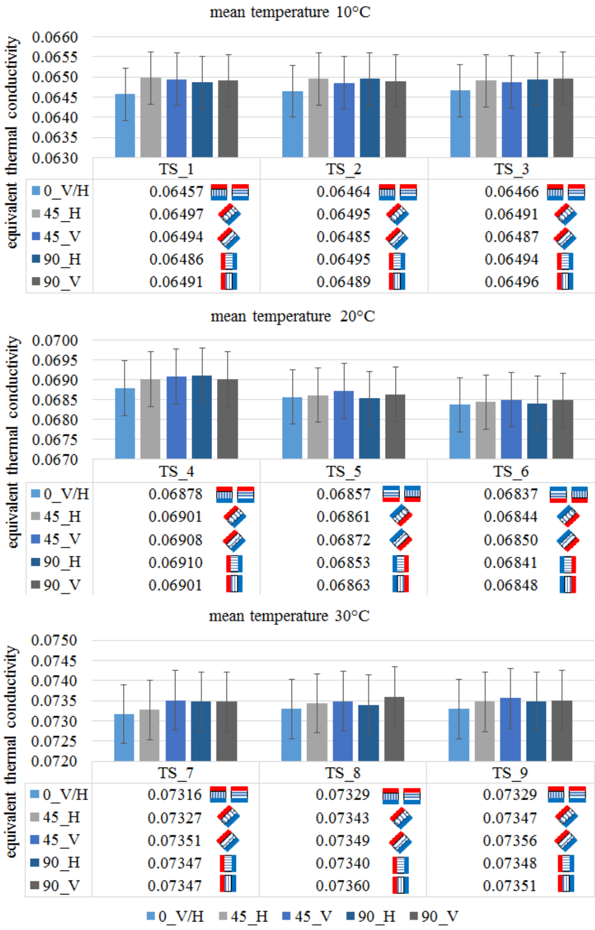

Fig. 4. Thermal conductivity results for PC25, mean temperatures 10 °C, 20 °C, 30 °C.

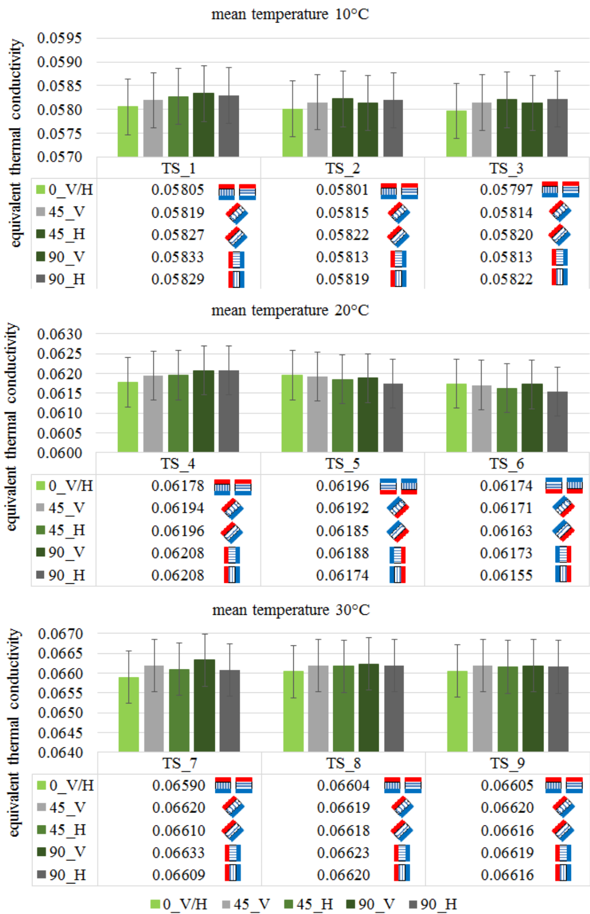

Fig. 5. Thermal conductivity results for PC32, mean temperatures 10 °C, 20 °C, 30 °C.

3.4 *Thermal performance analysis*

The results obtained from the measurements described in detail in Section 3.3, which were tested and presented separately for each setpoint, are transformed to a representative value for each mean temperature in this section. Because the temperature gradient (10 K, 20 K and 30 K) influences the equivalent thermal conductivity at the level of the fourth and sometimes even fifth decimal place, i.e. it is at a level of around 0.1%, the values stated in Table 4 represent the average value for all of the three gradients which together represent each mean temperature separately. The overall dependence of the equivalent thermal conductivity on the mean temperature is proved in accordance to the knowledge of the standard tests, which is represented by a conversion of thermal values. Based on results obtained from the mean temperature of 10 °C to 20°C, the conversion temperature coefficient is up to 0.0060 1/K (PC25) and 0.0063 1/K (PC32), while between the set of 20 °C and 30°C, it ranges for both samples at the same level, from 0.0065 1/K to 0.0069 1/K. In contrast, the angle of inclination of the sample (inclination 0°, 45° and 90°) and the orientation of the air cavities has hardly any influence on the equivalent thermal conductivity value for each measured mean temperature. The table also shows a comparison of results with those from the GHP method, which reaches higher equivalent thermal conductivity values for the tested panels. The difference in values ranges from 2.3% to 3.5%, which is practically a higher deviation than is acceptable according to the Keymark guidelines [36], however this represents a difference between both methods involved.

Table 4: Thermal conductivity results as an averaged value at three mean temperatures.

Test sample		PC25					PC32				
Test conditions and method		10 °C		20 °C		30 °C	10 °C		20 °C		30 °C
		λ_{eq}	F_T f_T	λ_{eq}	F_T f_T	λ_{eq}	λ_{eq}	F_T f_T	λ_{eq}	F_T f_T	λ_{eq}
0° HFM H		0.0646 ±0.0006	1.0619 0.0060	0.0686 ±0.0007	1.0671 0.0065	0.0732 ±0.0007	0.0660 ±0.0007	1.0655 0.0063	0.0618 ±0.0006	1.0680 0.0066	0.0660 ±0.0007
0° HFM V		0.0646 ±0.0006	1.0619 0.0060	0.0686 ±0.0007	1.0671 0.0065	0.0732 ±0.0007	0.0660 ±0.0007	1.0655 0.0063	0.0618 ±0.0006	1.0680 0.0066	0.0660 ±0.0007
45° HFM H	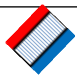	0.0649 ±0.0006	1.0601 0.0058	0.0688 ±0.0007	1.0683 0.0066	0.0735 ±0.0007	0.0661 ±0.0007	1.0610 0.0060	0.0618 ±0.0006	1.0696 0.0067	0.0661 ±0.0007
45° HFM V	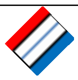	0.0649 ±0.0006	1.0586 0.0057	0.0687 ±0.0007	1.0684 0.0066	0.0734 ±0.0007	0.0662 ±0.0007	1.0636 0.0062	0.0619 ±0.0006	1.0695 0.0067	0.0662 ±0.0007
90° HFM H		0.0649 ±0.0006	1.0586 0.0057	0.0687 ±0.0007	1.0699 0.0068	0.0735 ±0.0007	0.0662 ±0.0007	1.0619 0.0060	0.0618 ±0.0006	1.0712 0.0069	0.0662 ±0.0007
90° HFM V		0.0649 ±0.0006	1.0586 0.0057	0.0687 ±0.0007	1.0699 0.0068	0.0735 ±0.0007	0.0663 ±0.0007	1.0636 0.0062	0.0619 ±0.0006	1.0711 0.0069	0.0663 ±0.0007
0° GHP n/a		0.0665 ±0.0020	1.0556 0.0054	0.0702 ±0.0021	1.0712 0.0069	0.0752 ±0.0022	0.0684 ±0.0020	1.0549 0.0053	0.0634 ±0.0019	1.0789 0.0076	0.0684 ±0.0020

Based on the experimental analysis it is proved that a difference in temperatures ranging from 10 K to 30 K do not have a significant effect on the results. However, the effect of a change in the mean temperature from 10 °C to 30 °C causes an increase in the relative value of approximately 12% in total. On the other hand (and quite surprisingly), the angle of inclination of the tested PC panels is found to have a very low or almost negligible effect on the equivalent value of thermal conductivity. The PC panels are characterized by quite small voids and not so different aspect ratios thus might the buoyancy effect in the convection heat transfer contribution to be considered almost negligible. A difference in values of only up to 1% is identified.

4 NUMERICAL CFD ANALYSIS

The further improvement of various currently available building materials, systems and components using optimization techniques, and their potential development, can be enhanced by applying suitable theoretical models. Experimental tests in conjunction with numerical computations can be used to validate and calibrate performance prediction models for building elements with the aim of conducting further optimization studies.

The main objective of the conducted numerical simulation was to verify results obtained experimentally on heat transfer through the studied PC panels under measured steady-state conditions. It primarily focused on the comparability of real and simulated results and the subsequent optimization of the novelty of panels improved with low-e modifications. In this idea, it is expected that their thermal performance will improve when the long-wave radiation and free convection are changed.

4.1*Modelling and simulation of polycarbonate models*

A model of the experimental set-up was created using the CFD simulation programme ANSYS Fluent [42]. Using the CFD method, which follows fundamental heat balance principles, makes it possible to model all the thermal and energy phenomena and fluid flows that occur within coupled transient radiation - natural convection heat transfer across PC panels subject to steady state boundary conditions. In this case the model is discretized and calculated using hexahedral, prismatic and pyramidal shapes.

The main parameters of the numerical CFD simulation employed to reproduce the experimental measurements are described in the following parts. The thermal performance of PC multi-wall panels was investigated at several temperature gradients and with variations in the angle of inclination of each test panel. Because the effect of various temperature gradients on the equivalent thermal conductivity was very low, only one particular gradient was finally used for further detailed analysis. The numerical CFD simulation was conducted using ANSYS software, version 14. A double parametric CFD numerical simulation was performed. The computational geometry was created in ANSYS Design Modeller software by coupling the fluid and solid regions of the simulated part. A periodically repeatable characteristic cross-section was considered to be the computational domain for each PC type. The internal walls of the PC panel (vertical or oblique) were modelled using the “shell conduction” method. The following PC computational domain lengths were tested: 60 cm, 120 cm and 240 cm. As the differences in the monitored results (thermal flows, flow velocities, the equivalent thermal conductivity of the PC panel) were negligible, the 60 cm-long computational domain was used for further analyses which corresponds to the measured panels.

The computational geometry was discretized by high quality hexahedral (predominantly structured) computational mesh using ANSYS Meshing software (Fig. 6).

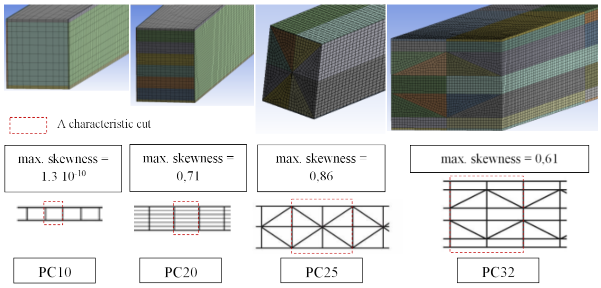

Fig. 6. Computational geometry and mesh

The independence of the results from the mesh was also verified by refining it three times. Dirichlet boundary conditions were set for the warm and cold side of the PC panel, while adiabatic boundary conditions were considered for the periodic planes. The air was considered to be an incompressible ideal gas. As it can be assumed that a very slow flow caused by natural convection will occur in the cavities of the PC panel - i.e. a flow at the boundary of the laminar and turbulent modes - the 3 equation turbulence transition model k-kl-ω was used for the simulation first. Subsequently, the 2 equation model k-ω SST was used for the same cases. As the congruence of the results obtained by both turbulence modelling methods was excellent, the computationally simpler k-ω SST model was used for further simulations. Second order discretisation schemes were used. The Discrete Ordinates (DO) radiation model was used for the simulation of heat transfer via IR radiation. The convergence criterion was assigned to a residual value of less than 10^{-6} in energy equation, as well as for continuity and air velocities. The count of iteration steps was greater than the 10^5 iteration for each parametric case.

4.2 *Results and discussion*

The measured equivalent thermal conductivity of all panels is compared in Table 3 for a particular temperature gradient of + 25 °C / -5 °C, which was used in test setpoint TS_3. Good congruence between the theoretical and experimental results is essential for the simulation model to be a reliable tool for the prediction of the overall thermal efficiency of PC panels of various structures and geometries. Table 5 shows the results from the numerical simulation of the basic model and a comparison with the measured data for panels in an angle of inclination

0° for the conditions of test setpoint TS_3. The difference in the results shows that in all cases very good congruence of up to 1% was achieved; sample PC25 achieved the highest difference, this being up to 1.8%.

Table 5: Thermal conductivity results; obtained consistency between the measured and simulated values for the base case models

Thermal conductivity	**PC10**	**PC20**	**PC25**	**PC32**
Average measured	0.06680	0.05280	0.06466	0.05797
Numerical simulated	0.06693	0.05239	0.06350	0.05756

4.3 *Effects of the angle of inclination and air cavity sizes*

The effect of the angle of inclination α was also analyzed in greater detail in terms of the each mechanism of the total heat transfer. As the effect of the inclination of the two tested panels with the most complex geometry showed small differences, a more detailed numerical analysis was carried out on a selected PC25 panel. The aim was to numerically clarify and partially identify the effect of the inclination on the combined heat transfer through the monitored system. The total heat flux q [W/m²] via conduction/convection and from radiation specifically in the PC25 panel is compared in Table 6. The radiation heat flux from the surface of the PC25 panel was simulated as being in the range from $q_{rad} = 25.24$ W/m² (α = 90°) to $q_{rad} = 26.49$ W/m² (α = 45°). However, the convection/conduction heat flux was obtained in the range from $q_{condv} = 49.59$ W/m² (α = 45°) to $q_{condv} = 51.10$ W/m² (α = 0°) (Table 6). This means that the radiation heat transfer roughly accounts for 50% of the overall heat transfer through this panel type. As can be seen, the overall heat flux as well as its radiation and convection/conduction components are practically the same. This is also visually demonstrated in Fig. 7, where air temperature fields are presented. However, the character and velocity of the natural flow in the cavities actually changes depending on the angle of inclination. At an angle of inclination of 90°, large vortices can be observed in the cavities of the PC. They spread throughout the whole length of the cavity – i.e., within the longitudinal section. The flow velocities are the greatest in this case because the largest dimension of the cavity points in the direction of the vector of gravitational acceleration. At an angle of inclination of 0°, small vortices form in the transverse cross section of the individual cavities and the flow velocity is the smallest out of the given cases as this time it is the smallest dimension of the cavity that points in the direction of the vector of gravitational acceleration. A combination of both effects occurs at an angle of inclination of 45°, when it is possible to observe pathlines which approximately take the shape of a helix, and a flow velocity which lies between the two previous marginal cases.

Table 6 Heat fluxes in the PC25 panel

	Heat Transfer	90°	45°	0°
PC25	Conduction /convection - q_{condv} [W/m²]	50.65	49.59	51.10
	Radiation - q_{rad} [W/m²]	25.24	26.49	25.18
	Total - q [W/m²]	75.89	76.08	76.28

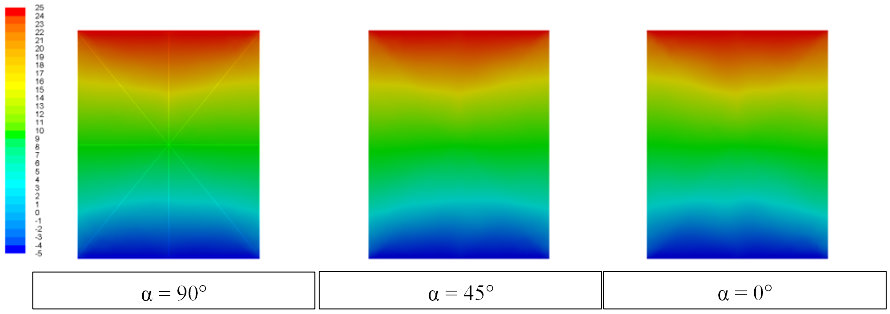

Fig. 7. PC25 The vertical cavity orientation - the effect of the angle of inclination. Air temperature [°C] in the cross section through the middle of the length of the cavity.

Another factor is the size of the studied panels in terms of their length, which can have a significant effect on the resultant heat transfer particularly through elements with air-filled layers. The aim is to demonstrate to what extent the size (or length) has an impact on the combined heat transfer via the air layers. Therefore, the results described above were subsequently subjected to an analysis which identified the influence of the size / length of the panel and / or the height of the air cavity on the resultant heat flow for three examined angles of inclination (α = 0°, 45° and 90°). Specifically, PC panel specimens with the following computational domain lengths were tested: 60 cm, 120 cm and 240 cm. The results of the simulation (Fig. 9) proved that the length of the air cavity has a negligible effect on the monitored results (thermal flows, flow velocity, equivalent thermal conductivity and angles of inclination), and so, as was stated before, a 60 cm long computational domain which corresponds with the experimental measurements was used for all analyses as well as for thermal optimization study with low-e application. The nature of the flow, as well as the distribution of temperatures, remains the same for all the evaluated lengths, as shown in Fig. 8.

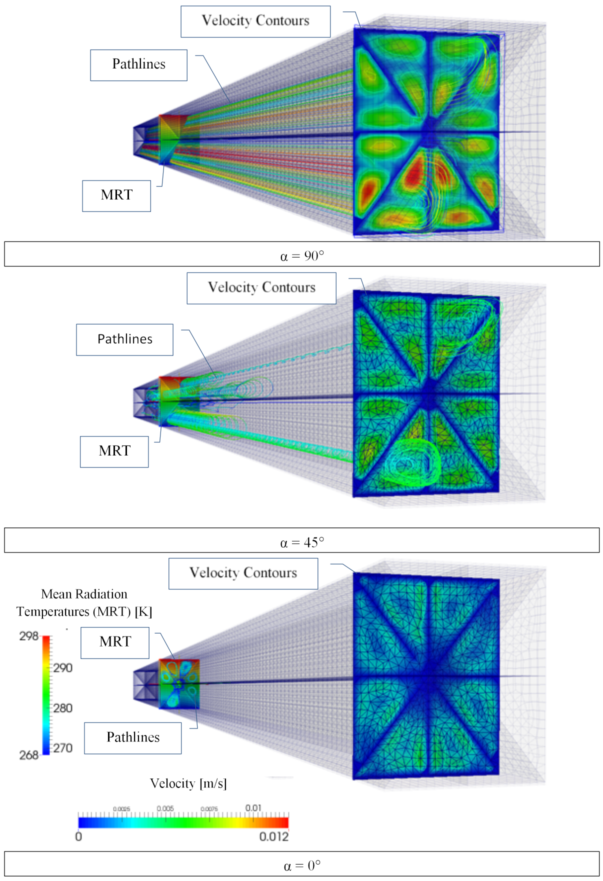

Fig. 8. PC25 The influence of PC vertical cavity orientation – the effect of the angle of inclination of longitudinal cavities from the horizontal direction on the natural convection - mean radiation temperature [K] and air flow velocity [m/s].

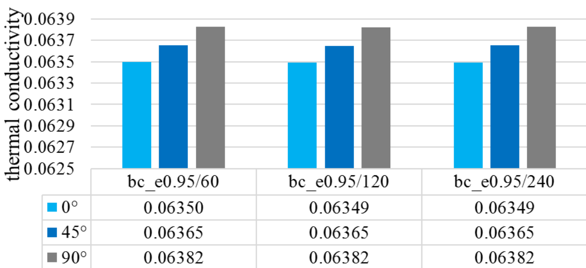

Fig. 9. Effects of different panel sizes/air cavity length on the equivalent thermal conductivity for PC25

5 THERMAL PERFORMANCE OPTIMIZATION

The use of design optimization techniques when investigating typical thermal engineering problems is an important tool for the improvement of existing systems. In the real world the integration of a more complex structure in the air cavity of a TIM can have a significant effect on the heat transfer via combined natural convection and radiation heat transfer through the investigated system. In order to comprehensively investigate the thermal characteristics of the low-e PC panels, a numerical three-dimensional CFD model was created and validated in the previous section as base case model.

5.1 *Low-e polycarbonate panels*

The PC panels that were measured experimentally, after verification via numerical modelling, were simulated in variants differing in the scale of low-e application, i.e. in whether low-e was applied to all or only selected surfaces of the internal walls of the investigated panels. Fig. 10 shows all of the simulated cases for each panel separately. The models with low-e application on various wall surfaces are highlighted using red lines.

The basic panel is the panel which was calculated during the verification of the measured experimental results using a numerical model, i.e. with an emissivity of 0.95 on all surfaces. This value was obtained experimentally to obtain real emissivity values of tested PC panels for use in numerical calculations. After the evaluation of the results of spectral reflectance analysis, the emissivity was found to be 0.95 and used for base case models. Variant 1 (v1) represents a scenario where all the surfaces of the internal walls have an emissivity of 0.1. Another variant 2 (v2) is where low-e was applied on all surfaces except for diagonal walls; in the case of PC10 and PC20, low-e is also not applied to walls running parallel to the direction of the heat flux. Variant 3 (v3) applies an emissivity of 0.1 to all of the internal walls running parallel to the external walls or those which are vertical to the direction of the heat flux. This means that in the case of diagonal walls or walls parallel to the direction of the heat flux (apart from PC10), the 0.95 emissivity of the basic model is used. Additionally, variant 4 represents a model for panels PC25 and PC 32 with low-e only on the outer walls inside and those walls which are perpendicular to them. The coefficients of the ratios between the non-treated and treated walls (6) and geometrical factors (GF) were derived from all of the variants. During this, the ratio between the sum of the lengths of all walls with low-e and the total area of the air cavities of a typical cross-section was considered according to formula (7). This represents the practical ratio between wall surfaces treated with low-e and the volume of air in contact with all of the internal walls, which analogously, has a character to the typical shape factor.

$$coef = \frac{\Sigma l_e}{\Sigma l} \qquad [-] \qquad (6)$$

$$GF = \frac{\Sigma l_e}{A_{ac}} \qquad [1/mm] \qquad (7)$$

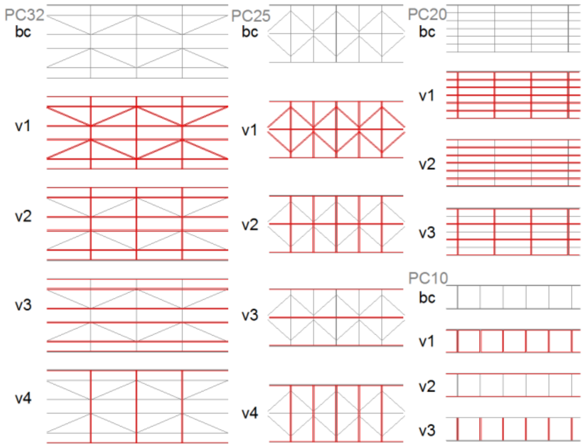

Fig. 10. Basic model with an emissivity of 0.95 and variant models (v1 to v4) with low-e application highlighted

Both factors were used to identify the dependence of the influence of low-e on the equivalent thermal conductivity. Table 7 shows calculated values in detail for the ratio of the sum of lengths with untreated (Σl) surfaces to that of treated surfaces with low-e (Σl_e), and also in relation to the total surface of the air cavities (A_{ac}) according to (5) in their typical cross-section.

Table 7: Geometrical factors derived based on the application of low-e

	PC10		A_{ac} 99.99	**PC20**		A_{ac} 331.1	**PC25**		A_{ac} 248.4	**PC32**		A_{ac} 638.4
	Σl_e	$\Sigma l_e /\Sigma l$	GF	Σl_e	$\Sigma l_e /\Sigma l$	GF	Σl_e	$\Sigma l_e /\Sigma l$	GF	Σl_e	$\Sigma l_e /\Sigma l$	GF
bc	0	-	0	0	-	0	0	-	0	0	-	0
v1	40.0	1.0	0.40	234.8	1.0	0.71	143.2	1.0	0.58	350.4	1.0	0.55
v2	19.8	0.49	0.20	193.8	0.82	0.59	89.8	0.63	0.36	263.5	0.75	0.41
v3	20.2	0.51	0.20	137.9	0.59	0.42	69.8	0.49	0.28	199.6	0.57	0.31
v4	n/a	n/a	n/a	n/a	n/a	n/a	39.8	0.28	0.16	103.8	0.30	0.16

5.2 *Simulation results and discussion*

The simulation model was validated based on experimental measurements presented in Section 4. The simulation model was calculated for several variants which differed exclusively in the application of low-e on particular walls of each panel. A situation was considered in which short-wave (solar) and long-wave (IR) thermal radiation from the outside had no influence on the tested PC samples. The thermal radiation is therefore realized only in the environment of PC panel cavities. Dirichlet boundary conditions were present on the warm and cold side of the PC panel. The Discrete Ordinates (DO) model of radiation was used for the simulation of heat transfer via IR radiation within the cavities. The air was considered to be completely diathermal. A relevant coefficient of emissivity was set for the internal surfaces.

As already mentioned concerning the parameters of the simulation described above, the results in this part were analyzed using CFD parametric numerical simulation. The obtained equivalent thermal conductivity values featuring the effect of low-e application on all or selected surfaces were compared graphically for the selected state of boundary conditions for a specific temperature gradient of + 25 °C / - 5 °C. In the first step, the effect of different emissivities applied to all internal surfaces was analyzed in greater detail for panel PC25. The results presented in the image below (Fig. 11a) show equivalent thermal conductivity values numerically obtained for the PC25 panel with an effect on different emissivities. Based on the results it can be stated that the change in emissivity has a greatly linear influence on the resultant values of equivalent thermal conductivity in all of the calculated positions. The effect of the change in emissivity from the basic value of 0.95 to 0.1 is demonstrated by the drop in the equivalent value from 0.0635 W / (m·K) to 0.04172 W / (m·K), which is a difference of approximately 34%. For an emissivity of 0.5, half efficiency is achieved. The graph shows a relation for the calculation of the equivalent value of thermal conductivity even in the case of a different emissivity value than the considered 0.95, 0.5 and 0.1. The results shown in the second part of the image (Fig. 11b) then show the differences for PC25 in all of the calculated variants together. Though an approximately 34% reduction in the equivalent value of thermal conductivity is achieved with the application of low-e on all internal walls (v1), under different conditions a gradually decreasing value of 27% (v2), 25% (v3) and 15% (v4) is achieved. This means that the difference between v2 and v3 is practically negligible, and that the application of lower emissivity on surfaces parallel to the total heat flux has an almost negligible effect.

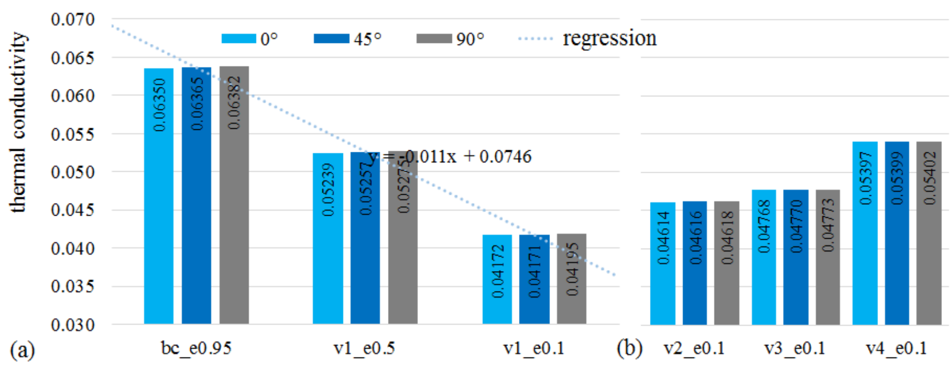

Fig. 11. PC25 (a) with changing emissivity effects and (b) at different low-e application ratios

The results shown in Fig. 12 record differences for the other calculated panels (PC10, PC20 and PC32) for the 0° position only. According to the calculated results, the application of low-e is the most effective for panel PC10 (Fig. 13a), for which the value is decreased by up to 43% from 0.06693 W / (m·K) to 0.03806 W / (m·K). This result roughly corresponds with the value achieved for the geometrically most complex panel, PC32. The application of low-e in variant 2 also achieves an acceptable reduction of up to 36%. On the other hand, panel PC20 has the lowest effect, reaching a maximum of 24%, which is mainly caused by the fact that its basic model already has a character with the lowest equivalent value, which significantly eliminates heat transfer via natural convection, and where the smallest cavity depth is 3.45 mm.

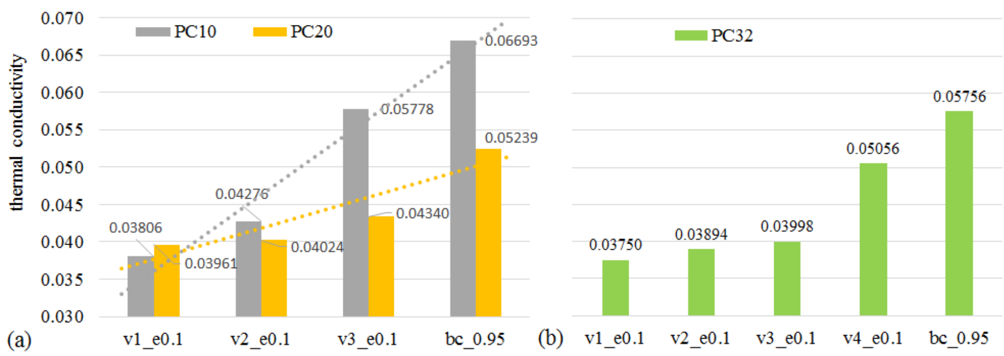

Fig. 12. Thermal performance of low-e panels (a) PC10 and PC20; (b) PC32

As in the case of PC25, PC32 has the greatest effect with regard to v1, reaching up to 35 %, meaning a change from the original value of 0.05756 W / (m.K) to 0.03750 W / (m.K). The other cases increase the effectiveness by 32 % (v2) and 31 % (v3), while with the last variant a maximum reduction of 12% is achieved. This means that a similar effect occurs and that the application of low-e only on internal surfaces which are perpendicular to the direction of heat flow (i.e. the situation in v3) is the most effective variant.

5.3 *Effects of low-e application on geometrical relations*

With regard to the evaluation of the results considering the range of application of low-e surfaces in the internal structures of the simulated PC panels, two proposed factors were employed with the aim of identifying the influence of the geometry and position of low-e surfaces on the resultant equivalent values for the thermal conductivity of used panels. The relationship between the two selected factors in Table 7 and all the calculated equivalent thermal conductivity values is expressed in Fig. 13 (the regressive functions are shown in the graphs). The ratio $\Sigma\, l_e \,/\, \Sigma\, l$ has almost a linear character with a decreasing function (Fig. 13a) for all data. On the other hand, the application of the low-e geometrical factor (GF) of the cross-section of the investigated panels means that if the ratio between just the surfaces with low-e applied and the total surface of the cross-section is considered, the decrease in the simulated values is exponentially more distinct.

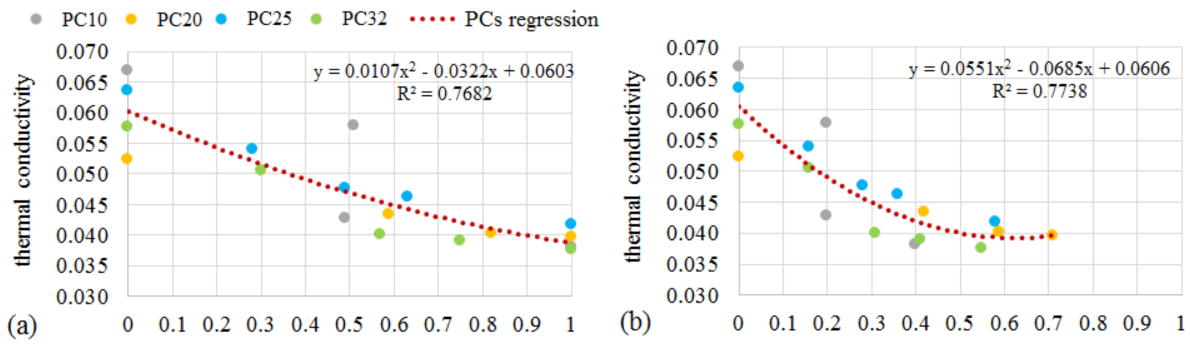

Fig. 13. Equivalent thermal conductivity results based on (a) wall to low-e wall ratio; (b) low-e geometrical factors (*GF*).

The results shown in Fig. 15 express the dependence of the equivalent thermal conductivity of multi-wall systems (PC20, PC25 and PC32) on the mean average thickness of the cavity (*MATC*) and simultaneously also on the ratio of this parameter to the total thickness of the examined panel (*MATC* / *d*). As the PC10 panel only has one typical rectangular cell and does not represent a system with multiple walls, it was not included in the result analyses related to the factors stated above. The results show (Fig. 14a) that the size of cavities only has an effect when they have no low-e surfaces. With the optimization of the development of these systems via the application of low-e, radiative heat transfer is a more important factor. In other words, when all internal surfaces are low-emission, the thickness of the PC panel and its division into cavities only has a small effect. Practically the opposite situation occurs when the mean average cavity thickness is in a relation with the total thickness of the system (Fig. 14b). The size of cavities with regard to the total thickness of the system has an effect on convective heat transfer and represents a stronger non-linearity with regard to the resultant equivalent thermal conductivity value.

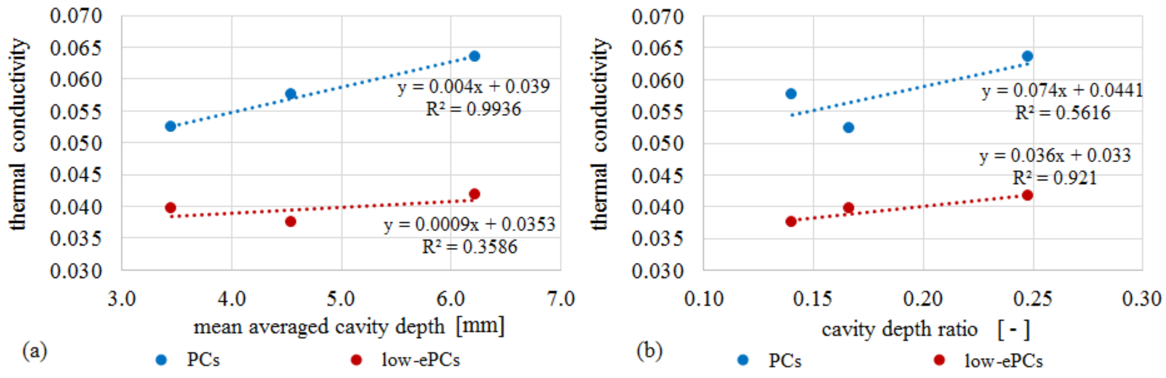

Fig. 14. Equivalent thermal conductivity results based on (a) mean averaged cavity depth (*MACT*) and (b) its weighting with regard to the overall thickness (*MATC/d*).

6 CONCLUSION

The study presents a detailed thermal analysis of polycarbonate (PC) panels using both experimental and numerical simulation methods. The aim was to theoretically improve the thermal performance of these systems with low-e application.

The experimental results are analysed in order to identify the dependence of equivalent thermal conductivity on the temperature and angle of inclination. Based on the experimental analysis it was identified that a difference in temperatures ranging from 10 K to 30 K did not have a significant effect on the results. However, the effect of a change in the mean temperature from 10 °C to 30 °C was demonstrated by a conversion of thermal values with the temperature conversion coefficient of approximately 0.006 1/K. On the other hand, the angle of inclination of the tested polycarbonate panels was found to have a very low or almost negligible effect on the equivalent value of thermal conductivity. A difference in values of only up to 1% was recorded that is in the range of the measurement uncertainty. This effect was subsequently investigated in detail using a numerical CFD simulation which showed that the nature and speed of natural flow changes in cavities depending on the angle of inclination but has a practically negligible effect on the individual components of heat transfer and combinations of them expressed by the equivalent value of thermal conductivity.

The created CFD simulation models of the basic PC panels with standard surface emissivity were validated successfully using experimental measurements. A good agreement was found between the numerical results and experimental data. The maximum deviation (i.e. 1.8%) is for the PC25 panel. This resulted in the further use of the numerical model for the quantification of the influence of low-e effect on the equivalent thermal conductivity of the modified PC panels. The results show that affecting the longwave radiative heat transfer significantly decreases the equivalent thermal conductivity of PC panels and low-e application is very effective in improving the thermal performance of the PC panels. Depending on the type of the PC panel, the equivalent thermal conductivity was reduced by an amount ranging from 24 % (0.03961 W/(m·K) for PC20) to 43 % (0.03806 W/(m·K) for PC10). In this relation, several geometrical dependencies on the equivalent thermal conductivity of the PC panels modified with low-e was also introduced to identify the effect of their different geometries and panel thickness. The equivalent thermal conductivity decreases with both wall to low-e wall ratio and low-e geometrical factors. However, when the relation to the cavity thickness is analysed, the thickness of the PC panel and the way it is divided into cavities has only a small effect on the equivalent thermal conductivity.

Based on the findings from this study, it will be possible to initiate further testing with the aim of investigating the real effect of low-e interactions on the improvement of the thermal performance of PC panels. In such case, recent technological advances and the technical possibilities of the application of low-e in PC systems need to be adopted for further research efforts. One production way can be based on application of proper conducting polymers in liquid or aqueous solution form that are able to be highly transparent. In relation to this, further research should be carried out regarding detailed optical properties in the visible region as well as effect on the solar transmittance parameters.

ACKNOWLEDGEMENT

This research was supported by Czech Science Foundation in Czechia, project GA 20-00630S "Climate responsive components integrated in energy and environmentally efficient building envelope", and by project No. VEGA 1/0680/20 supported the Scientific Grant Agency of the Ministry of Education, Science, Research and Sport of the Slovak Republic . Special thanks to J. Zach and R. Slávik with their technical contribution in performing the experiments is appreciated here.

Nomenclature

Symbol:	Expression	Unit
A	Area	[m^2]
d	Thickness	[m]
F_T	Temperature conversion factor	[-]
f_T	Temperature conversion coefficient	[1/K]
l	Length	[m]
T_{up}	Upper plate temperature	[°C]
T_{low}	Lower plate temperatures	[°C]

T_m	Mean temperature	[°C]
ΔT	Temperature gradient	[K]
q	Specific heat flow	[W]
R	Thermal resistance coefficient of measured element	[m^2.K/W]
U	Heat transfer coefficient of measured element	[W/(m^2.K)]
ΔT	Temperature gradient	[K]
Greek symbols		
α	angle	[°]
λ	Lambda, thermal conductivity	[W/(mK)]
Abbreviations and subscripts:		
a	Air	
c	Cavity	
conv	Convection	
cond	Conduction	
CFD	Computational fluid dynamics	
Eq	Equation	
eq	Equivalent	
GF	Geometrical factor	
GHP	Guarded heat plate	
H	Horizontal	
HFM	Heat flow meter	
LW	Longwave radiation region	
m	Mean	
PC	Polycarbonate	
rad	Radiation	
sim	Simulation, simulated	
TC	Test condition	
TIM	Transparent insulation material	
TS	Test setpoint	
V	Vertical	

REFERENCES

[1] B.P. Jelle, S. E. Kalnæs, T. Gao, Low-emissivity materials for building applications: A state-of-the-art review and future research perspectives, *Energy Build*. 96 (2015) 329-356.

[2] S. B. Sadineni, S. Madala, R. F. Boehm, Passive building energy savings: A review of building envelope components, *Renew. Sust. Energ. Rev.* 15(8) (2011) 3617-31.

[3] M. Čekon, J Čurpek, A transparent insulation façade enhanced with a selective absorber: A cooling energy load and validated building energy performance prediction model, *Energy and Build.* 183 (2019) 266-282.

[4] A. Paneri, I.L. Wong, S. Burek, Transparent insulation materials: An overview on past, present and future developments, *Sol. Energy* 184 (2019) 59-83.

[5] Y. Sun, Y. Wu, R. Wilson, Analysis of the daylight performance of a glazing system with Parallel Slat Transparent Insulation Material (PS-TIM), *Energy Build*. 139 (2017) 616-633.

[6] H. Omrany, A. Ghaffarianhoseini, A. Ghaffarianhoseini, K. Raahemifar, J. Tookey, Application of passive wall systems for improving the energy efficiency in buildings: A comprehensive review, *Renew. Sust. Energ. Rev.* 62 (2016) 1252–1269.

[7] J.D. Osorio, A. Rivera-Alvarez, P. Girurugwiro, S. Yang, R.Hovsapian, J.C. Ordonez, Integration of transparent insulation materials into solar collector devices. *Sol. Energy* 147 (2016) 8–21.

[8] H. Kessentini, J. Castro, R. Capdevila, A. Oliva, Development of flat plate collector with plastic transparent insulation and low-cost overheating protection system, *Appl. Energy* 133 (2014) 206-223.

[9] K. Struhala, M. Čekon, R. Slávik, Life Cycle Assessment of Solar Façade Concepts Based on Transparent Insulation Materials. *Sustainability* 10 (2018) 4212.

[10] M. Čekon, K. Struhala, Polycarbonate multi-wall panels integrated in multi-layer solar façade concepts. *IOP Conf. Ser. Mater. Sci. Eng*. 415 (2018) 012055.

[11] I.L. Wong, P.C. Eames, R.S. Perrera, A review of transparent insulation systems and the evaluation of payback period for building applications. *Sol. Energy* 81 (2016) 1058–1071.

[12] Y. Sun, R. Liang, Y. Wu, R. Wilson, P. Rutherford, Glazing systems with Parallel Slats Transparent Insulation Material (PS-TIM): Evaluation of building energy and daylight performance, *Energy Build.* 159 (2018) 213-227.

[13] C. Buratti, E. Moretti, Lighting and energetic characteristics of transparent insulating materials: experimental data and calculation, *Indoor Built Environ.* 20(4) (2011) 400-411.

[14] E. Moretti, M. Zinzi, E. Belloni, Polycarbonate panels for buildings: Experimental investigation of thermal and optical performance, *Energy Build.* 70 (2014) 23-35.

[15] M. Čekon, R. Slávik, J. Zach, Experimental Analysis of Transparent Insulation Based on Poly-carbonate Multi-Wall Systems: Thermal and Optical Performance, *Energy Procedia* 132 (2017) 502-507.

[16] C. Buratti, E. Moretti, Transparent insulating materials for buildings energy saving: experimental results and performance evaluation, *Third International Conference on Applied Energy*, May 2011, Perugia, Italy, 2011, 1421-1432.

[17] E. Moretti, M. Zinzi, E. Carnielo, F. Merli, Advanced Polycarbonate Transparent Systems with Aerogel: Preliminary Characterization of Optical and Thermal Properties, *Energy Procedia* 113 (2017) 9-16.

[18] U. Berardi, The development of a monolithic aerogel glazed window for an energy retrofitting project, *Appl. Energy* 154 (2015) 603-615.

[19] C. Buratti, E. Moretti, Experimental performance evaluation of aerogel glazing systems, *Appl. Energy* 97 (2012) 430-437.

[20] P. Jelle, Traditional state-of-the-art and future thermal building insulation materials and solutions – properties, requirements and possibilities. *Energy Build.* 43 (2011) 2549-2563.

[21] E Cuce, P.M. Cuce, J.C. Wood, S.B. Riffat Toward aerogel based thermal superinsulation in buildings: a comprehensive review, *Renew. Sust. Energ. Rev.* 34 (2014) 273-299.

[22] S. Fantucci, F. Goia, M. Perino, V. Serra, Sinusoidal response measurement procedure for thermal performance assessment of PCM by means of Dynamic Heat Flow Meter Apparatus, *Energy Build.* 183 (2019) 297-310.

[23] H. Elarga, S. Fantucci, V. Serra, R. Zecchin, E. Benini, Experimental and numerical analyses on thermal performance of different typologies of PCMs integrated in the roof space, *Energy Build.* 150 (2017) 546-557.

[24] Q. Cai, H. Ye, Q. Lin, Analysis of the optical and thermal properties of transparent insulating materials containing gas bubbles, *Appl. Therm. Eng.* 100 (2016) 468-477.

[25] S. Fantucci, V. Serra, Experimental Assessment of the Effects of Low-Emissivity Paints as Interior Radiation Control Coatings, *Appl. Sci.* 10 (2020) 842.

[26] S. Fantucci, V. Serra, Low-E paints enhanced building components: Performance, limits and research perspectives, *Energy Procedia* 126 (2017) 274-281

[27] P. Principi, R. Fioretti, Thermal analysis of the application of pcm and low emissivity coating in hollow bricks, *Energy Build*. 51 (2012) 131-142.

[28] R. Fioretti, P. Principi, Thermal Performance of Hollow Clay Brick with Low Emissivity Treatment in Surface Enclosures, *Coatings* 4 (2014) 715-731.

[29] Z. Svoboda, M. Kubr, Numerical simulation of heat transfer through hollow bricks in the vertical direction, *J. Build. Phys.* 34(4) (2011) 325–350.

[30] G. Baldinelli, F. Bianchi, S. Gendelis, A. Jakovics, G. Luca Morini, S. Falcioni, S. Fantucci, V. Serra, M.A. Navacerrada, C. Díaz, A. Libbra, A. Muscio, F. Asdrubali, Thermal conductivity measurement of insulating innovative building materials by hot plate and heat flow meter devices: A Round Robin Test, *Int. J. Therm. Sci.* 139 (2019) 25-35.

[31] M. Montiel-González, J.F. Hinojosa, H.I. Villafán-Vidales, A. Bautista-Orozco, C.A. Estrada, Theoretical and experimental study of natural convection with surface thermal radiation in a side open cavity, *Appl. Therm. Eng.* 75 (2015) 1176-1186.

[32] D. K. Singh, S.N. Singh, Combined free convection and surface radiation in tilted open cavity, *Int. J. Therm. Sci.* 107 (2016) 111-120

[33] H. Karatas, T. Derbentli, Three-dimensional natural convection and radiation in a rectangular cavity with one active vertical wall, *Exp Therm Fluid Sci.* 88 (2017) 277-287.

[34] information on http://www.arlaplast.com/cs/products/polycarbonate-multiwall/

[35] CEN - EN 12667 (2001) *Thermal Performance of Building Materials and Products - Determination of Thermal Resistance by Means of Guarded Hot Plate and Heat Flow Meter Methods - Products of High and Medium Thermal Resistance*, p. 58

[36] ISO 8302:1991, *Thermal insulation - Determination of steady-state thermal resistance and related properties - Guarded hot plate apparatus*, International Organization for Standardization (ISO): Geneva, Switzerland, 1991, p. 47.

[37] ISO 8301:1991. *Thermal insulation -- Determination of steady-state thermal resistance and related properties -- Heat flow meter apparatus*, *(ISO 8301:1991)*. International Organization for Standardization (ISO): Geneva, Switzerland, 1991; p. 38.

[38] E. Rasmussen, C. Stacey, A. Koenen, E.L.W. Kurkinen, Comparative testing of thermal conductivity for thermal insulation products – the European Keymark experience for more than 50 equipment at 25 test institutes, 32nd International Thermal Conductivity Conference 20th International Thermal Expansion Symposium April 27–May 1, Purdue University, West Lafayette, Indiana, USA, 2014.

[39] U. Berardi, M. Naldi, The impact of the temperature dependent thermal conductivity of insulating materials on the effective building envelope performance, *Energy Build*. 144 (2017) 262-275.

[40] S. Fantucci, A. Lorenzati, A. Capozzoli, M. Perino, Analysis of the temperature dependence of the thermal conductivity in Vacuum Insulation Panels, *Energy Build.* 183 (2019) 64-74.

[41] ISO 10456:2007, *Building materials and products — Hygrothermal properties — Tabulated design values and procedures for determining declared and design thermal values*, International Organization for Standardization (ISO): Geneva, Switzerland, 2007, p. 25.

[42] ANSYS FLUENT Theory Guide, Ansys Help System: Release 14.0. (2011). https://support.ansys.com/portal/site/AnsysCustomerPortal (accessed February 26, 2019).